The Astrophysical Journal Letters, 927:L15 (6pp), 2022 March 1 https://doi.org/10.3847/2041-8213/ac5520

Core Electron Heating by Triggered Ion Acoustic Waves in the Solar Wind

F. S. Mozer[1,2], S. D. Bale[1,2], C. A. Cattell[3], J. Halekas[4], I. Y. Vasko[1], J. L. Verniero[5], and P. J. Kellogg[3]
[1] Space Sciences Laboratory, University of California, Berkeley, CA, USA
[2] Physics Department, University of California, Berkeley, CA, USA
[3] University of Minnesota, Minneapolis, MN, USA
[4] University of Iowa, Iowa City, IA, USA
[5] Goddard Space Flight Center, Greenbelt, MD, USA
Received 2021 November 13; revised 2022 February 14; accepted 2022 February 15; published 2022 March 7

Abstract

Perihelion passes on Parker Solar Probe orbits 6–9 have been studied to show that solar wind core electrons emerged from 15 solar radii with a temperature of 55 ± 5 eV, independent of the solar wind speed, which varied from 300 to 800 km s^{-1}. After leaving 15 solar radii and in the absence of triggered ion acoustic waves at greater distances, the core electron temperature varied with radial distance, R, in solar radii, as $1900R^{-4/3}$ eV because of cooling produced by the adiabatic expansion. The coefficient, 1900, reproduces the minimum core electron perpendicular temperature observed during the 25 days of observation. In the presence of triggered ion acoustic waves, the core electrons were isotropically heated as much as a factor of two above the minimum temperature, $1900R^{-4/3}$ eV. Triggered ion acoustic waves were the only waves observed in coincidence with the core electron heating. They are the dominant wave mode at frequencies greater than 100 Hz at solar distances between 15 and 30 solar radii.

Unified Astronomy Thesaurus concepts: Solar corona (1483); Solar wind (1534)

1. Introduction

Ion acoustic waves have been observed by many satellites in the solar wind (Gurnett & Anderson 1977; Gurnett & Frank 1978; Kurth et al. 1979; Lin et al. 2001; Mozer et al. 2020; Pisa et al. 2021). They are wideband waves of short duration that differ greatly from the triggered ion acoustic waves seen at 15–30 solar radii on the Parker Solar Probe (PSP) (Mozer et al. 2021), in that these latter waves are narrowband waves of long duration (hours to days) that often appear as shock-like bursts of 100–1000 Hz waves whose bursts are phase-locked with low-frequency ion-acoustic-like waves. The purpose of this paper is to study the effects of these triggered ion acoustic waves on the electron plasma. It has long been known that the core solar wind electrons must be heated as they move away from the Sun (Hartle & Sturrock 1968) to overcome some of the temperature loss associated with their adiabatic expansion, but the heating mechanism has not previously been identified in experimental data. The role of ion acoustic waves in this heating has been discussed theoretically (Dum 1978) and via calculations (Kellogg 2020). This paper will further examine their role as a mechanism for electron heating, thereby addressing the science goal of the PSP mission, to "trace the flow of energy that heats ... the solar corona and solar wind" (Fox et al. 2016). The FIELDS (Bale et al. 2016; Malaspina 2016; Mozer et al. 2020B) and SWEAP (Halekas et al. 2020; Kasper et al. 2016; Whittlesey et al. 2020) instruments on the Parker Solar Probe obtained the data presented in this paper.

A gas expanding into the void cools as it expands. To derive an expression for this cooling, it is assumed that PV^{γ} is constant, where $P = nkT_E$ is the plasma pressure, n is the density, V is the gas volume, and $\gamma = 5/3$ for a monatomic gas. Since $n \propto R^{-2}$ and $V \propto R^2$, where R is the distance from the Sun, these equations combine to yield a core electron perpendicular temperature that varies with radius as $R^{-4/3}$ in the absence of in situ heating . Orbits 6–9 were fit to a radial profile of the form $1900R^{-4/3}$ eV, where the coefficient, 1900, produced the minimum temperature observed on the 25 observation days. In the following discussion, the observed perpendicular temperature will be compared with this minimum temperature to determine locales where electron heating may have occurred. Other than in Figure 5, all figures give only the core perpendicular temperature (and not the parallel temperature) because the two temperatures are essentially equal (see Figure 5) so the parallel temperature is omitted for clarity.

2. Data

Figure 1 presents data from the perihelia of orbits 6 and 8. Panels 1A and 1G give the electric field spectra, panels 1B and 1H give the core perpendicular electron temperature in black and the minimum temperature, $1900R^{-4/3}$ eV, in red, panels 1C and 1I give the ion perpendicular temperature, panels 1D and 1J give the solar wind speed, panels 1E and 1K give T_E/T_I, and panels 1F and 1L give the spacecraft distance from the Sun in units of solar radii. Halekas et al. (2020) provided the electron temperature data shown throughout this paper.

As seen in panel 1A, there were two types of wave activity: the broadband, normal ion acoustic waves of short duration that appear as vertical lines and the narrowband waves of longer duration at the beginning of the interval, which lasted for times ~1 hr, and which are the triggered ion acoustic waves. Expanded examples of each of these waves are given in Figure 2. Panel 2A illustrates the spectrum of the triggered ion acoustic waves that were present at early times in Figure 1(A). As shown, they are narrowband waves that existed in this case for times of the order of an hour. They occurred in regions where T_E/T_I was large (panel 2B) and the electron temperature of panel 2C exceeded the minimum temperature, $1900R^{-4/3}$ eV, by more than a factor

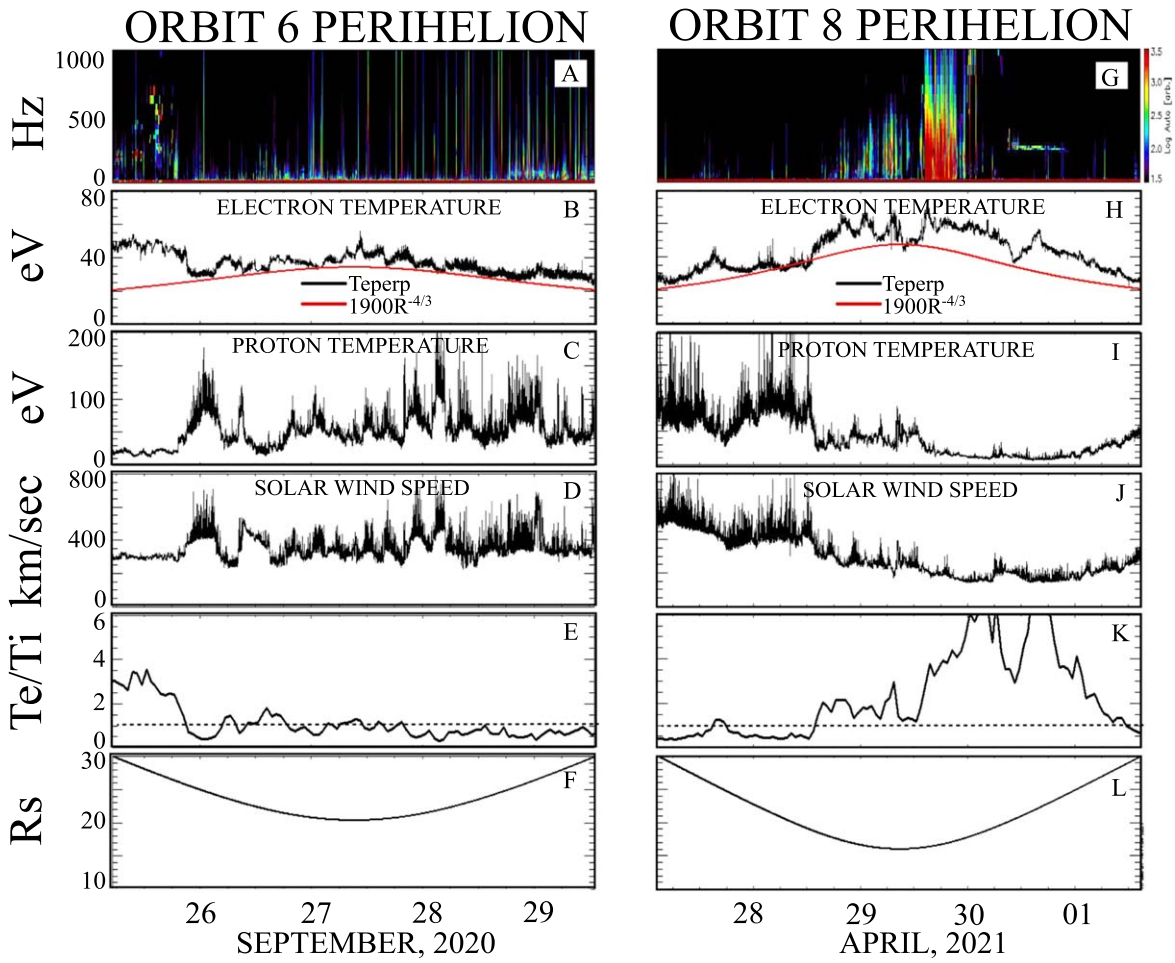

Figure 1. Plasma parameters during perihelion passes 6 and 8 of the Parker Solar Probe. Note that after the first day of orbit 6, the electron temperature followed the red curve of minimum temperature even though the solar wind speed varied from 300 to 800 km s^{-1}.

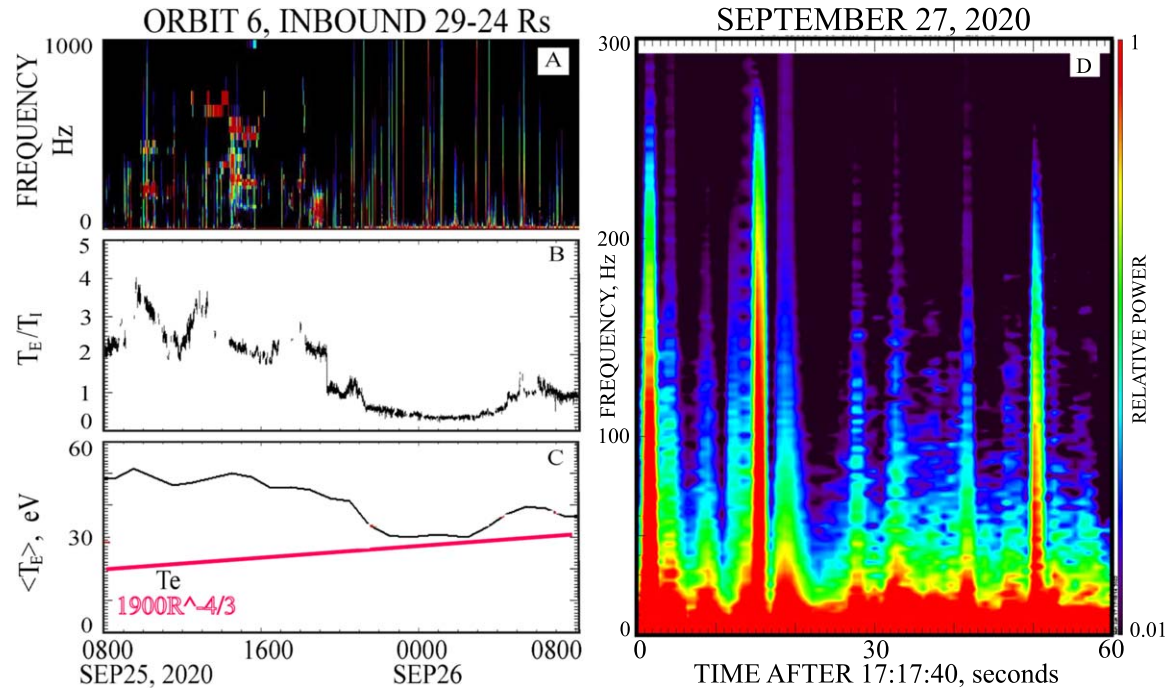

Figure 2. Triggered and normal ion acoustic waves observed during orbit 6. The triggered ion acoustic waves (panel 2A) were associated with large T_E/T_I (panel 2B) and heated electrons (panel 2C). Note that the triggered ion acoustic waves were narrowband in frequency and of long duration (hours) while the normal ion acoustic waves during the one minute interval of panel 2D were broadband waves of short duration.

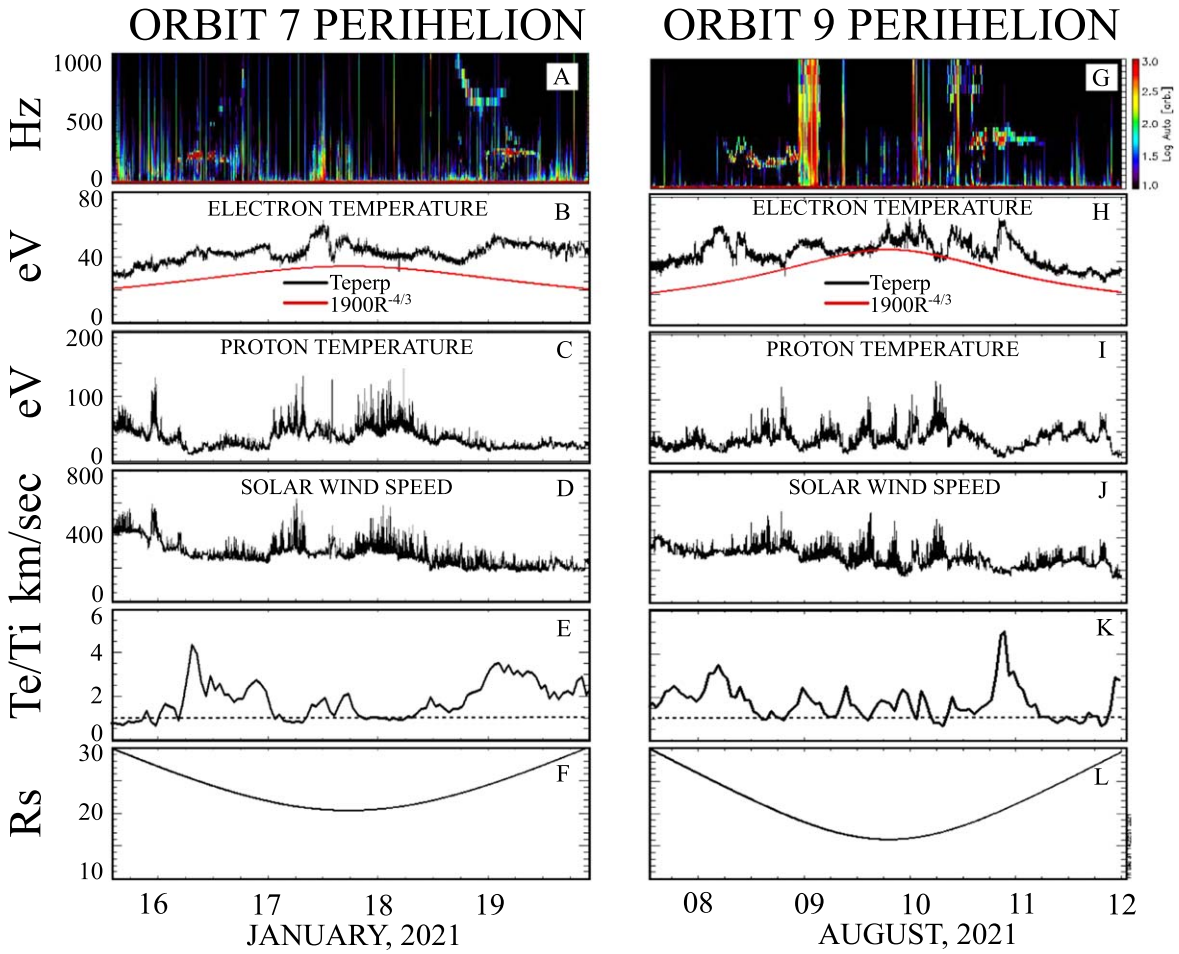

Figure 3. Plasma parameters during perihelion passes 7 and 9 of the Parker Solar Probe. Note that the electron temperature was approximately equal to but not less than the red curve of minimum temperature in the absence of waves, and that it exceeded the red curve by as much as a factor of two near triggered ion acoustic waves.

of two. The one minute of data in panel 2D illustrates the normal ion acoustic waves that were broadband structures lasting for times of the order of seconds.

The electron temperature of panel 1B exceeded the minimum temperature curve of $1900R^{-4/3}$ for two reasons. One reason was the 10%–20% temperature increases due to the weak anticorrelation of the temperature with the solar wind speed during days 26–29 of Figure 1(B) when the solar wind speed varied from 300 to 800 km s^{-1} and the only observed waves were the normal ion acoustic waves. The second reason was the increase in temperature by a factor of more than two in the first day of data in panel 1B in the presence of triggered ion acoustic waves, also illustrated in Figures 2(A) and (C).

The dependences of the electron temperature described above also occurred during orbit 8 in panels 1G–1L. Early in the interval and at occasional later times, the temperature of panel 1H was near the red curve in the absence of triggered ion acoustic waves and in the presence of small T_E/T_I, while at other times the temperature greatly exceeded the red curve of minimum temperature during periods of triggered ion acoustic waves. Recall that the red curve describes the lowest electron temperature observed during the two passes in Figure 1, as well as in Figure 3 for perihelia 7 and 9. Thus, the summary of the data in Figures 1 and 3 is that, in the absence of triggered ion acoustic waves, the electron temperature was greater than the minimum temperature by ∼10%–20%, while it exceeded the minimum temperature by as much as a factor of two during periods of triggered ion acoustic waves.

Figures 4(A)–(H) provide expanded views of two intervals between 21 and 30 solar radii in orbit 7 when the triggered ion acoustic waves (and some normal ion acoustic waves) were observed. Looking from perihelion outward in either direction, the red curves in Figures 4(C) and (G) show the decrease in minimum temperature expected from adiabatic expansion. After perihelion, in panel 4G, the temperature further increased above the minimum temperature to signify that there was a significant increase in core electron perpendicular temperature (the black curve in panel 4G) at the time of the triggered ion acoustic wave in panel 4E. Before perihelion, in panel 4C, there is a smaller increase in temperature at the time of the triggered ion acoustic waves. Each of these curves is a one-hour running averages made from about 500,000 raw data points.

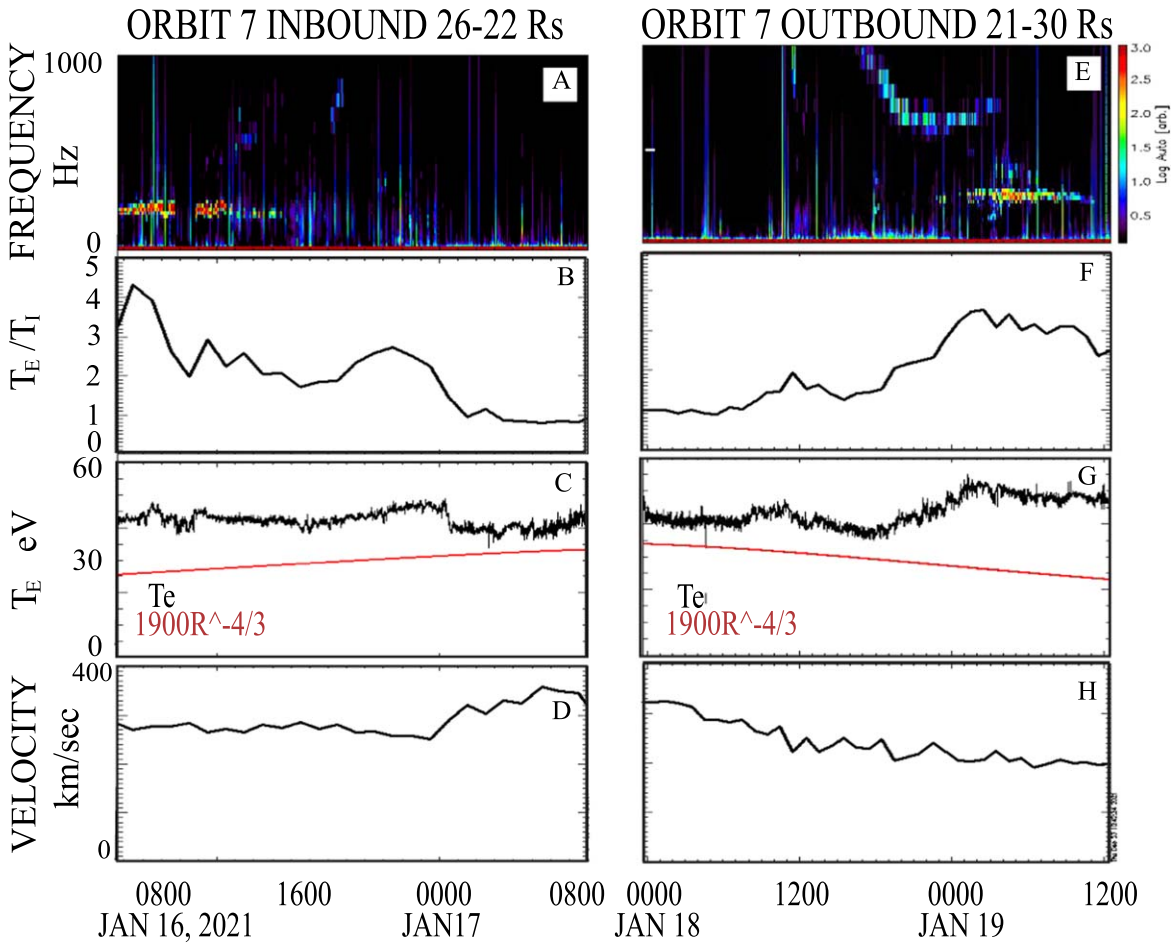

Figure 4. The inbound (panels 4A–4D) and outbound (panels 4E–4H) passes of orbit 7, illustrating the electric field, temperature ratio, electron temperature, and the plasma velocity. The red curves of minimum temperature in panels 4C and 4G give the decreases in electron temperature with distance expected for adiabatic expansion of the electron gas without heating. Their differences from the measured temperatures (the black curves) show that electrons were heated in regions containing triggered ion acoustic waves (panels 4A and 4E) and large ratios of electron to ion temperature (panels 4B and 4F).

Mixing of spatial and temporal variations is illustrated in Figures 4(A) and (C), where heated electrons were also observed at lower altitudes (later times) when there were no triggered ion acoustic waves. This situation can result from electrons heated by waves at a lower altitude than the satellite location, such that the heated electrons arrived at the spacecraft before or in the absence of the slower moving waves. Thus, one cannot expect a detailed one-to-one correlation between the waves and the heating but there should be a general correlation, such as that shown during all of the heating events.

Figure 5 gives the electron and ion temperatures versus radial distance, obtained from combining the data of orbits 6–9 into a single file as a function of radial distance and performing a one-hour running average of these data. The left panel shows that core electron heating occurred between 20 and 25 solar radii because the core perpendicular and parallel electron temperatures rose above the red curve of minimum temperature between 20 and 25 solar radii and they remained above that curve at larger radial distances. Each plot consists of some 10,000,000 raw data points.

Because the ion temperature at 15 solar radii was strongly dependent on the solar wind speed (see Figures 1 and 3), it is not possible to determine the ion heating as a function of radial distance from the available data (right panel of Figure 5) without correction of the dependence of the ion temperature on the solar wind speed.

Whistler waves are not seen in the region of 20–25 solar radii (Cattell et al. 2022).

Triggered ion acoustic waves are distinguished from normal ion acoustic waves by their narrowband frequency and longer duration, which may be understood (Kellogg 2022). Very often, but not always, the triggered ion acoustic waves have the following properties (see Figure 6), which are not understood theoretically;

1. An electric field wave of a few hertz is present, accompanied by bursts of waves of a few hundred to

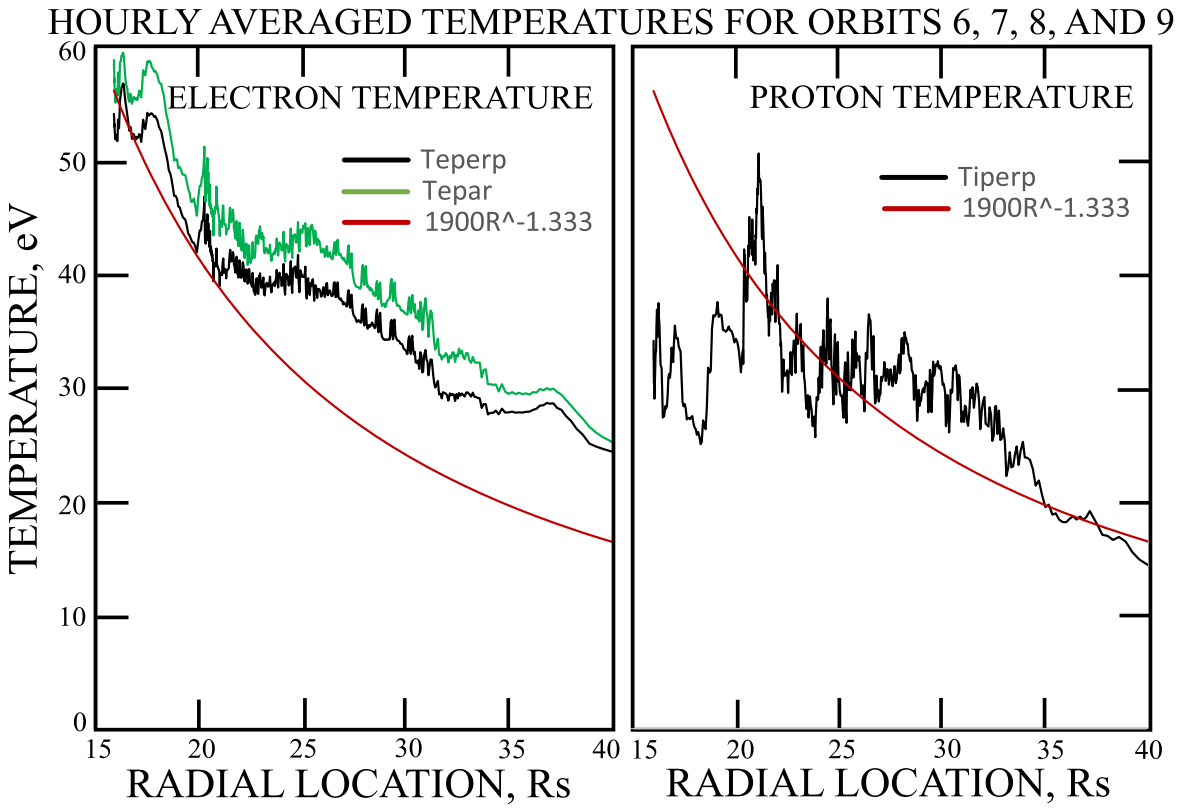

Figure 5. The core electron and ion temperatures vs. solar radius, as determined from the eight passes of the Parker Solar Probe through the region of 15–40 solar radii on orbits 6–9. Each curve gives the one-hour running average of some 10,000,000 raw data points. The red curves of minimum temperature give the radial variation of the temperature for adiabatic expansion with no heating. The deviation between the core electron temperatures and the red curve in the left panel shows that electrons were heated in the region of 20–25 solar radii. Because the ion temperature depended much more strongly on the solar wind speed than did the electron temperature, it is not possible to determine the ion heating in the right panel without correcting for the dependence of the ion temperature on the solar wind speed.

1000 Hz whose bursts are phase-locked with each low-frequency period (Figure 6(A)).
2. These periodic field structures can exist for large fractions of a day (see Figure 4 of Mozer et al. 2021).
3. Plasma density fluctuations of a few hertz and a few hundred hertz (determined from the spacecraft potential) are present at the two frequencies (Figures 6(B) and (C)).
4. No magnetic field signature is observed at either of these two wave frequencies (Figure 6(D)).
5. The higher frequency electric field and density fluctuations are pure sine waves, indicating that the waves are very narrowband (Figures 6(E) and (F)).

3. Discussion

The summary, from the statistics available on the altitude range of 15–30 solar radii during four orbits (eight passes, three of which are shown in detail in Figures 2 and 4), is:

1. there were two passes with $T_E/T_I \leqslant 1$, few waves, and no electron heating.
2. there were six passes with $T_E/T_I > 1$, with triggered ion acoustic waves, and with correlated core electron heating.

The conclusions drawn from this limited data set are:

1. in the absence of triggered ion acoustic waves, the core electron perpendicular temperature was 10%–20% greater than the minimum temperature of $1900R^{-4/3}$ (51–61 eV at 15 solar radii) in spite of variations in solar wind speed from 300 to 800 km s^{-1}.
2. in the presence of triggered ion acoustic waves, the electron temperature increased by as much as a factor of two above the minimum temperature, $1900R^{-4/3}$ eV.

These findings are consistent with the hypothesis that triggered ion acoustic waves contribute to core electron heating in the inner heliosphere.

Future PSP orbits will investigate the triggered ion acoustic waves to provide further statistics on their occurrence and their electron heating. They will also provide higher frequency measurements of plasma density fluctuations (through measurements of the spacecraft potential), which may be a significant contributor to electron heating and to achieving

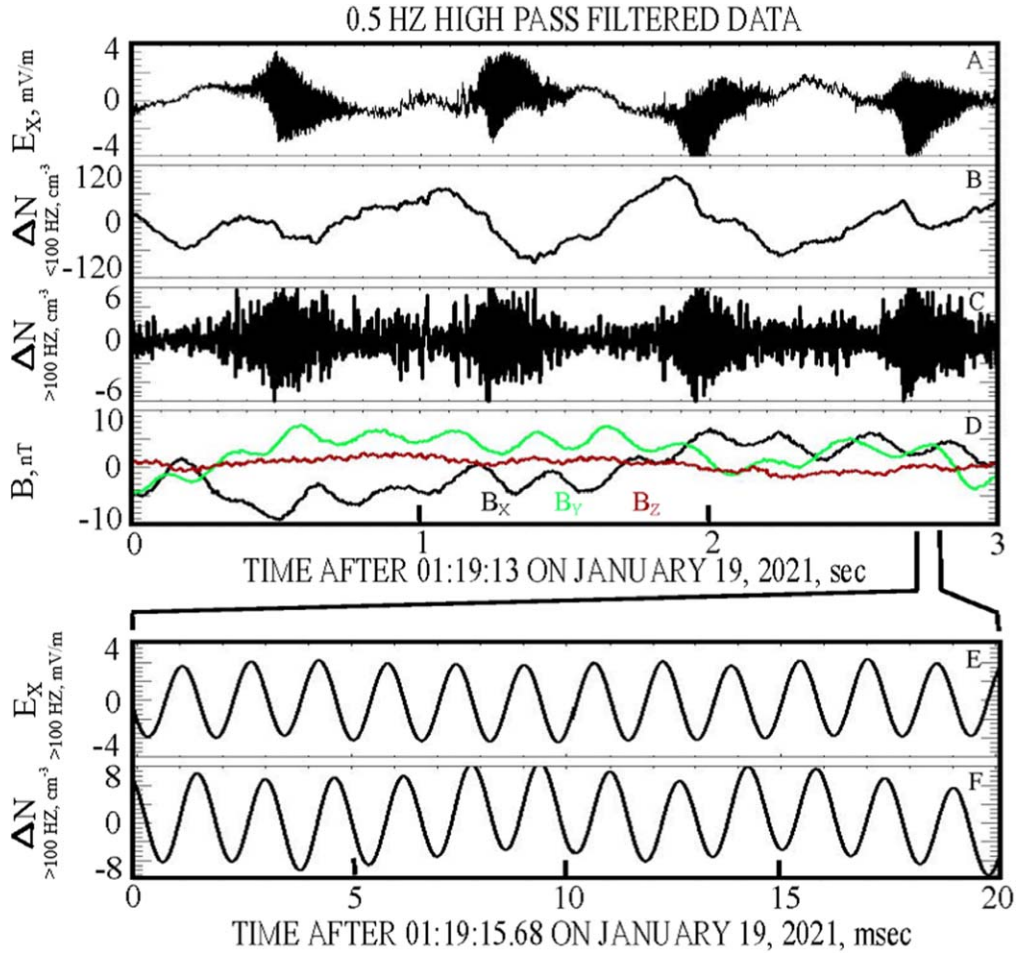

Figure 6. Features of triggered ion acoustic waves, including the electric field having higher frequency pulses in phase with a wave of a few hertz (panel 6A), low- and high-frequency density fluctuations in sync with the electric fields (panels 6B and 6C), the absence of magnetic field signatures of a similar frequency (panel 6D), and with the higher frequency electric field and density fluctuations being narrowband signals (panels 6E and 6F).

the PSP mission goal of assessing the dominant mechanisms of energy exchange and plasma heating near the Sun.

This work was supported by NASA contract NNN06AA01C. The authors acknowledge the extraordinary contributions of the Parker Solar Probe spacecraft engineering team at the Applied Physics Laboratory at Johns Hopkins University. The FIELDS experiment on the Parker Solar Probe was designed and developed under NASA contract NNN06AA01C. Our sincere thanks to P. Harvey, K. Goetz, and M. Pulupa for managing the spacecraft commanding, data processing, and data analysis, which has become a heavy load thanks to the complexity of the instruments and the orbit. We also acknowledge the SWEAP team for providing the plasma data. The work of I.V. was supported by NASA Heliophysics Guest Investigator grant 80NSSC21K0581

ORCID iDs

F. S. Mozer https://orcid.org/0000-0002-2011-8140
S. D. Bale https://orcid.org/0000-0002-1989-3596
C. A. Cattell https://orcid.org/0000-0002-3805-320X
J. Halekas https://orcid.org/0000-0001-5258-6128
I. Y. Vasko https://orcid.org/0000-0002-4974-4786
J. L. Verniero https://orcid.org/0000-0003-1138-652X
P. J. Kellogg https://orcid.org/0000-0001-5223-689X

References

Bale, S. D., Goetz, K., Harvey, P. R., et al. 2016, SSRv, 204, 49
Cattell, C., Breneman, A., Dombeck, J., et al. 2022, ApJ, 924, L33
Dum, C. T. 1978, PhFl, 21, 945
Fox, N. J., Velli, M. C., Bale, S. D., et al. 2016, SSRv, 204, 7
Gurnett, D. A., & Anderson, R. R. 1977, JGR, 82, 632
Gurnett, D. A., & Frank, L. A. 1978, JGR, 83, 1
Halekas, J. A., Whittlesey, P., Larson, D. A., et al. 2020, ApJS, 246, 22
Hartle, R. E., & Sturrock, P. A. 1968, ApJ, 151, 1155
Kasper, J. C., Abiad, R., Austin, G., et al. 2016, SSRv, 204, 131
Kellogg, P. J. 2020, ApJ, 891, 51
Kellogg, P. J. 2022, ApJ, 925, 106
Kurth, W. S., Gurnett, D. A., & Scarf, F. L. 1979, JGR, 84, 3413
Lin, N., Kellogg, P. J., Macdowall, R. j., & Gary, S. P. 2001, SSRv, 97, 193
Malaspina, D. M. 2016, JGRA, 121, 5088
Mozer, F. S., Agapitov, O. V., Bale, S. D., et al. 2020B, JGRA, 125, e27980
Mozer, F. S., Bonnell, J. W., Bowen, T. A., Schumm, G., & Vasko, I. V. 2020, ApJ, 901, 107
Mozer, F. S., Vasko, I. Y., & Verniero, J. L. 2021, ApJL, 919, L2
Pisa, D., Soucek, J., & Santolik, O. 2021, A&A, 656, A14
Whittlesey, P. L., Larson, D. E., Kasper, J. C., et al. 2020, ApJS, 246, 74